Journal of Petroleum Science and Technology, Vol. 2, No. 2, 2012, 40-49

An Experimental Study of the Effect of High Electric Field on Mass Transfer Enhancement

R. Karami*, M. Ayazi, L. Samiee, M. Dehghani Mobarake, and F. Goodarzvand-chegini
Development and Optimization of Energy Technologies Research Division, Research Institute of Petroleum Industry (RIPI)
karamir@ripi.ir

Abstract
Applying corona wind as a novel technique can lead to a great level of heat and mass transfer augmentation by using a very small amount of energy. The enhancement of forced flow evaporation rate by applying electric field (corona wind) has been experimentally evaluated in this study. Corona wind produced by a fine wire electrode charged with positive high DC voltage impinges on water surface and leads to an evaporation enhancement by disturbing the saturated air layer over water surface. The study was focused on the effect of corona wind velocity, electrode spacing, and air flow velocity on the level of the evaporation enhancement. Two sets of experiments, i.e. with and without electric field, have been conducted. The data obtained from the first experiment were used as a reference for the evaluation of the evaporation enhancement in the presence of electric field. The applied voltages ranged from corona threshold voltage to spark over voltage with increments of 1 kV. The results shows that corona wind has a great enhancement effect on water evaporation rate, but its effectiveness gradually diminishes by increasing air flow velocity. The maximum enhancements are 7.3 and 3.6 times for air velocities of 0.125 and 1.75 m.s^{-1} respectively.

Keywords: Electrohydodynamics (EHD), Corona Wind, High Electric Field, Evaporation Enhancement

Introduction
It is well known that when air flows over a body of water, a thin layer of relatively inert air exists on the surface of water. This saturated air layer interferes with the diffusion of water molecules from water surface to the bulk air flow. As the air velocity over the surface falls, the thickness of saturated air layer increases and evaporation rate degrades; thus, any methods which can disturb this boundary layer might improve evaporation rate. Applying electrohydrodynamic can enhance water evaporation substantially with producing a secondary air flow called corona wind. To practice this, a high voltage is applied between two electrodes. In this method, a moist material is placed on the surface of a flat electrode. Corona wind impinges on the surface of the material and disturbs the saturated air layer, which leads to an evaporation enhancement. When a dielectric placed in an electrostatic field, three forces act on it and they are determined by Equation 1 [1].

$$\mathbf{F}_e = q_e\mathbf{E} - \frac{\varepsilon_0}{2}E^2\nabla\varepsilon + \frac{\varepsilon_0}{2}\nabla\left(E^2\frac{d\varepsilon}{d\rho_a}\rho_a\right) \quad (1)$$

The first term on the right hand side of the equation is called Coulomb force and represents a volumetric electrostatic force which is connected with the presence of free electric charges (q_e) in a dielectric fluid. The second term results from the non-uniformity of dielectric constant ($\nabla\varepsilon$) in a fluid volume subjected to an electric field. The third term deals with an electrostrictive phenomenon and represents forces acting on a dielectric in a non-uniform electric field. The first term of EHD forces is the main force which contributes to an evaporation enhancement and single phase heat transfer augmentation [2]. The second and the third terms are important in two-phase heat transfer where differences in temperature and density cause variation in electric permittivity [3, 4].

Although several studies have demonstrated the feasibility of EHD-enhanced evaporation [5-9], some effective parameters in this technique need more studies. In this paper, the effects of electric field intensity, primary air flow velocity, and electrode spacing are investigated and correlations for the evaporation enhancement and EHD performance are presented.

Corona Wind Theory and Velocity

The electric corona discharge usually occurs when a high electric voltage is applied between two electrodes with substantially different radii of curvature. For this purpose, highly curved electrode could be a needle or a small diameter wire and the other electrode could be a flat plate or a cylinder. High intensity electric field in the vicinity of the sharp electrode causes air around it to break down partially and become a conductor. Under this condition, air is ionized and results in a corona discharge. Corona discharge could be positive or negative. This is determined by the polarity of voltage on the sharp electrode with respect to the flat electrode. There are always a very small amount of free electrons in the surrounding air. In a positive corona, electrons are attracted toward the corona electrode (sharp electrode) and positive ions are propelled to the flat electrode by Coulomb force. As the positive ions travel toward the flat electrode, they collide with neutral air molecules and exchange momentum. The result is an ion-drag flow from the sharp electrode to the flat one. This flow is also called corona wind or ionic wind [12]. It should be noted that the direction of corona wind flow is from the sharp electrode to the flat one regardless of its electrode polarity.

Electrode geometry used in this research was wire-plate electrodes. If it is assumed that wire electrode is located at x=0 and at a distance of L from the plate electrode, there will be a very small bipolar region with a radius of x_0 formed around the wire electrode where positive and negative ions drag in opposing directions; so, its contribution to a net ion-drag flow is negligible and could be eliminated from the calculations. Electric field distribution between two plate electrodes (E) is obtained from Equation 2 [13].

$$E^2 - E_0^{\,2} = \frac{2I(x - x_0)}{Ab\varepsilon_0} \tag{2}$$

where, E_0, I, A, b, and ε_0 are electric field intensity between two plate electrodes, electric current between two electrodes, area of flat electrode, ion mobility of positive ions, and electric permittivity of free space respectively. Since average electric field between wire and plate electrode is equal to E_0, which represents a uniform electric field between two plate electrodes with a voltage and distance of V and L respectively ($E_0 = \frac{V}{L}$), Equation 2 is applicable for wire-plate electrode geometry using average electric field. With the assumption that a complete momentum transfer from ionic space charges (q_e) to the air bulk take place, the conservation law of energy could be written as follow:

$$\frac{1}{2}\rho_a U_e^{\,2} = \int_{x=x_0}^{x=L} q_e E \, dx \tag{3}$$

In this equation, ρ_a is air density.

Combining Equations 2 and 3, and using the Guass law ($\nabla . E = \frac{q_e}{\varepsilon_0}$), corona wind velocity (U_e) approximation under the wire electrode reads:

$$U_e = \sqrt{\frac{2IL}{\rho_a Ab}} \tag{4}$$

The detailed derivation steps are given elsewhere [14].

Experimental Setup and Procedure

Experimental setup used for the present study is shown schematically in Figure 1. The main components are a rectangular wind tunnel, an air box, a blower, a personal computer, a high voltage DC power supply, two temperature/humidity data loggers and a velocity vane anemometer. Wind Tunnel was made of Plexiglas with the dimensions of 220×20×9.5 cm. An air box with converging section contained two series of honeycomb structures fixed in two different sections, placed at the inlet of the tunnel to produce a uniform airflow in the test section. In this study, eight different air velocities (i.e. 0.125, 0.25, 0.5, 0.75, 1.0, 1.25, 1.5, and 1.75 $m.s^{-1}$) were used. The air velocity in the wind tunnel was controlled using a damper with a sliding door situated at the outlet of the blower and one could control the air speed into the test section by adjusting the opening of the sliding door. Water container was mounted on the base of the wind tunnel. It was measured 70 cm long, 20 cm wide, and 1 cm deep and made of Plexiglas except for its base which was made of copper plate as the plate electrode. A cooper wire as the corona emitting electrode with the radius of 77 μm was suspended horizontally along the water surface with the same length of the water container and parallel to the air flow. In order to investigate the effect of corona wire spacing from the plate electrode on the evaporation enhancement, wire to plate spacing was made adjustable (i.e. 3, 4, 5, and 6 cm). In order to measure the dry bulb temperature and relative humidity of air at the outlet of wind tunnel more accurately, an orifice was located inside the wind tunnel at a distance of 45 cm downstream of water container to mix water vapor and bulk air flow. DC voltage was applied to the wire electrode using a high voltage power supply (Heinzinger PNC 40000-5) within the range of 0 to 40 kV and 0 to 5 mA. the evaporation rate of water was determined by measuring dry the bulb temperature and relative humidity of air at the inlet and outlet sections of the wind tunnel using a temperature/humidity data logger (Testo 177 H1). The velocity of air flow through the wind tunnel was measured by an anemometer (Testo 435) equipped with a vane probe at the outlet section of the wind tunnel.

All experiments were carried out in pairs (with and without electric field). In each experiment, the air flow rate was set at a specific value. The first experiment was performed in the absence of electric field and the evaporation rate was determined in the presence of air flow alone. Immediately after that, the second experiment was carried out by applying the electric field and air flow simultaneously.

The applied voltage was increased from corona inception voltage to a voltage close to the breakdown limit with increments of 1 kV; however, for voltages below 10 kV, the increments were selected to be 0.5 kV.

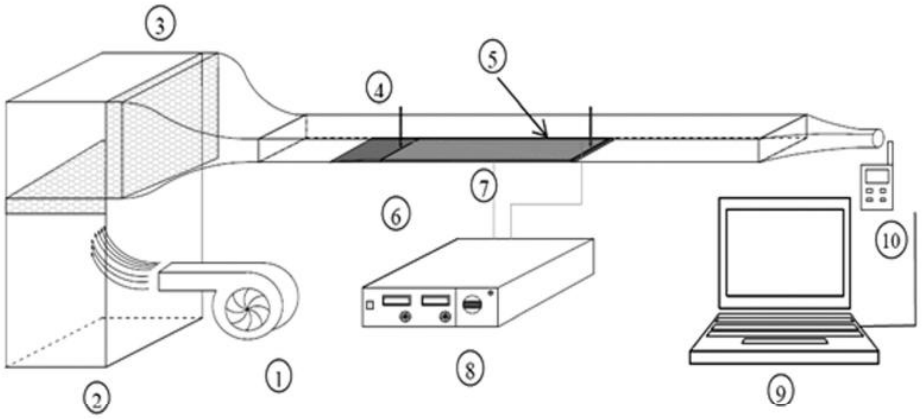

Figure 1: The experimental setup: (1): Blower; (2): Air box; (3): Honeycomb; (4): Wind tunnel; (5): Wire electrode; (6): Plate electrode; (7): Water container; (8): HV Power supply; (9): Computer; (10): Temperature/humidity data logger

The results obtained from the first experiment which was conducted in the presence of air flow alone were used as a reference in the evaluation of the evaporation enhancement value by electric field. The level of water in the container was kept constant at 1 cm in all the experiments. This procedure was repeated for different air velocities as well as different electrode spacings.

Data Reduction

As it was noted before, the relative humidity and dry bulb temperature of air were measured at the inlet and outlet sections of the wind tunnel. These data were used for the evaluation of humidity ratio of air (ω) using the following thermodynamic relation:

$$\omega = 0.622 \frac{\phi\, p_g}{p - \phi\, p_g} \tag{5}$$

where, φ is the relative humidity measured directly by the temperature/humidity data logger; p is the atmospheric pressure of air and pg stands for the saturated pressure of water vapor calculated at a measured temperature.

Evaporation rate was determined based on the difference between the water content of the inlet and outlet air flow from the wind tunnel

$$\dot{m}_{eva} = \dot{m}_{dry\,air} \times (\omega_2 - \omega_1) \tag{6}$$

Mass flow rate of dry air $(\dot{m}_{dry\,air})$ was obtained by measuring the mean velocity of air (U) through the wind tunnel as follows:

$$\dot{m}_{dry\,air} = \rho_a \times U \times A_w \tag{7}$$

In this equation, A_w is cross sectional area of the wind tunnel.

Sherwood number, which is a dimensionless number and resembles Nusselt number in heat transfer, was used to express the evaporation rate and is defined as its conventional form:

$$Sh = \frac{h_m d}{D} = \left(\frac{\dot{m}_{eva}}{A \Delta C}\right) \frac{d}{D} \tag{8}$$

where, A is the surface area of water, the same as the plate electrode area and d is the characteristic length taken as the length of the water container. D stands for the mass diffusivity of water vapor into bulk air flow and its value was found using Equation 9. Mass diffusivity of water vapor is a function of air pressure *(P)* and the temperature of water surface *(T)* which is equal to the wet bulb temperature of inlet air flow to the wind tunnel and is calculated based on measured dry bulb temperature and the relative humidity of air at the inlet section of the wind tunnel.

$$D = 2.26 \times 10^{-5} \left(\frac{101325}{P}\right)\left(\frac{T}{273.15}\right) \tag{9}$$

ΔC is the difference in water vapor concentration between the water surface and bulk air flow. The value of water vapor concentration was calculated from the following equation:

$$C = \rho_a\, \omega \tag{10}$$

Results and Discussion

In this paper, the data obtained from the evaporation experiments are cast in the form of Sherwood number and are presented as the ratio of Sherwood number in the presence of electric field and air flow simultaneously *(Sh)* to the Sherwood number in the presence of air flow alone (Sh_0). The effect of electric field on the water evaporation enhancement for two different air velocities *(U)* and four electrode spacings *(L)* is shown in Figure 2.

Although all the experiments were carried out for air flow velocities of 0.125, 0.25, 0.5, 0.75, 1.0, 1.25, 1.5, and 1.75 $m.s^{-1}$, here the results are only presented for the two limiting air velocities (i.e. U=0.125 and 1.75 $m.s^{-1}$).

In this figure, the evaporation enhancement is plotted versus applied voltage. Each plot corresponds to a fixed air flow velocity, with electrode spacing appearing as a changing parameter.

It is shown that for all the electrode spacings, the evaporation enhancement increases by increasing the applied voltage.

This could be attributed to the corona wind velocity. The higher the electric field strength is, the more air ionization happens, which leads to more collisions and faster corona wind velocity.

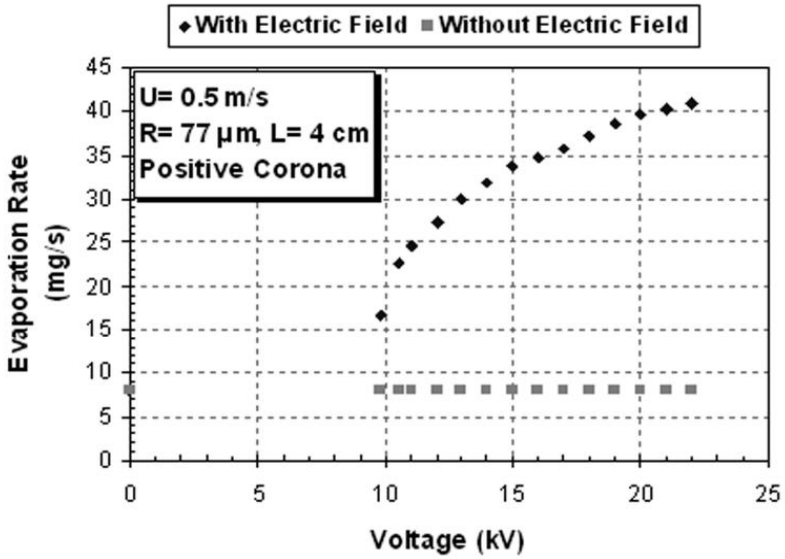

Figure 2: Absolute evaporation rate versus voltage

The higher the electric field strength is, the more air ionization happens, which leads to more collisions and faster corona wind. It should be noted that for a fixed air flow velocity, the maximum enhancement is nearly equal and independent of electrode spacing except for the least electrode spacing (*L= 2* cm) at which an early breakdown voltage inhibits a further increase of voltage and avoids reaching a higher value of enhancement.

As it was expected, for a fixed voltage, lower electrode spacings show a greater enhancement. This happens because of electric field intensification and an increase in the corona wind velocity. Also, a rise in electrode spacing postpones corona inception voltage as well as breakdown voltage.

For having a better understanding of the effect of applying high electric field on mass transfer enhancement, the absolute evaporation rate versus electric voltage is plotted in Figure 3 and compared with the case that no electric field is applied. As it is shown, evaporation rate has improved considerably in the presence of a high electric field.

Moreover, if one compares the two plots in Figure 3, it can be concluded that an increase in air flow velocity leads to a decrease in the level of the evaporation enhancement. To consider this behavior more accurately, the value of the evaporation enhancement at different air flow velocities are compared at a fixed electrode gap in Figure 4.

Each plot corresponds to a fixed electrode spacing, while the air flow velocity ranges from 0.125 to 1.75 $m.s^{-1}$. The results for the two limiting electrode spacings, namely 3 and 6 cm, are presented in this figure. For both electrode spacings, the effect of corona wind on the evaporation enhancement was suppressed by increasing air flow velocity. In this work, the maximum enhancement ranged from 7.3 to 3.6 at L= 4 cm, as the air velocity increased from 0.125 to 1.75 $m.s^{-1}$.

It can be deduced that air flow velocity has an inverse effect on the evaporation enhancement in the presence of electric field. The ions produced in the vicinity of the wire electrode are less effective in exchanging momentum to fast moving neutral air molecules when the air flow velocity is high. Another explanation is that at high air flow velocities, saturated boundary layer over the water surface is thin and the evaporation rate is already high and hence corona wind disturbance cannot enhance the evaporation rate much further; but, at low air velocities, saturated layer is thick and any disturbance in this layer can lead to a significant evaporation enhancement.

In addition to the decrease in the evaporation enhancement by increasing air flow velocity, it can be seen that at low air flow velocities, the increase in the evaporation enhancement is steep and nonlinear at low voltages whereas it becomes linear at higher voltages; but as air flow velocity increases, the slope of the variation of the evaporation enhancement moderates gradually and becomes nearly linear.

The results show that corona wind velocity as a cross flow (Ue) and axial air flow velocity (U) are two effective parameters which respectively have a direct and inverse relationship to the evaporation enhancement level.

Thus, to evaluate the enhancement in water evaporation for the cases with the simultaneous presence of electric field and air flow, a dimensionless number can be defined as EHD number which is the ratio of corona wind velocity (as defined in Equation 4) to the air flow velocity.

$$N_{EHD} = \frac{U_e}{U} \quad (11)$$

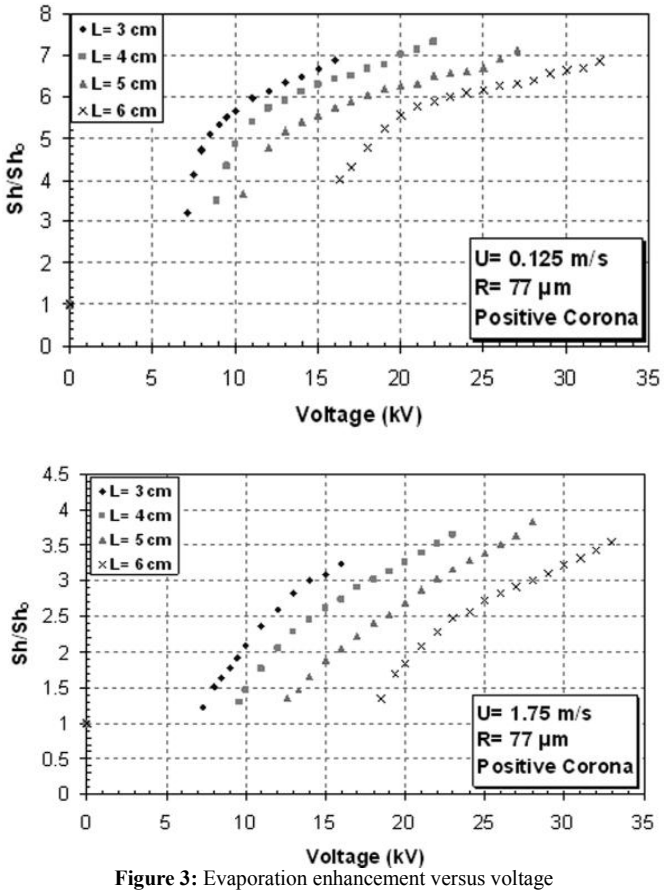

Figure 3: Evaporation enhancement versus voltage

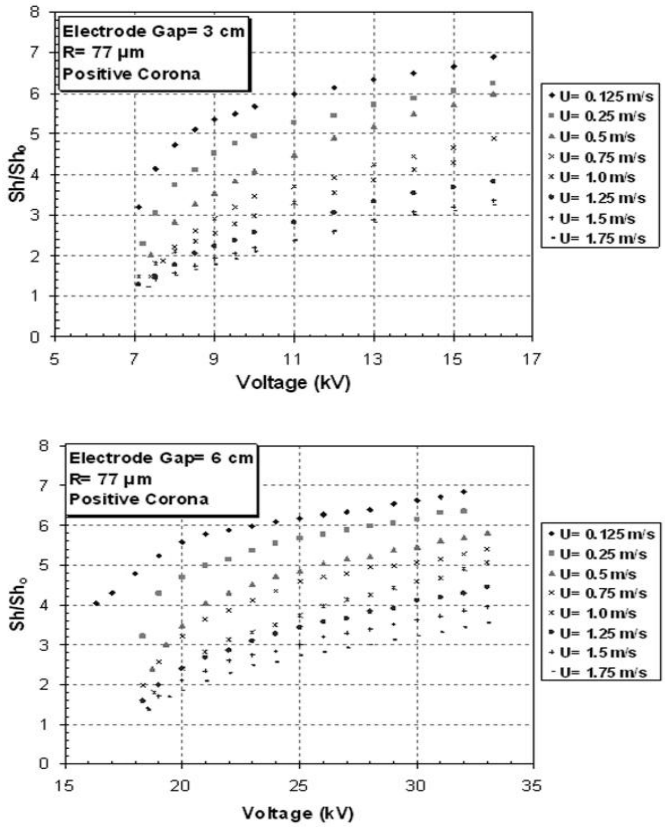

Figure 4: Evaporation enhancement versus voltage for different air velocities

The EHD number defined above is equivalent to the square root of the force ratio (Ion-drag force/ inertial force) defined by Sadek [15].

Figure 5 shows the evaporation enhancement as a function of EHD number for two limiting air velocities, namely 0.125 and 1.75 $m.s^{-1}$, and different electrode spacings. As it was expected, in each plot, the value of the evaporation enhancement is nearly independent of electrode spacing and it is only a function of corona wind velocity for a fixed EHD number.

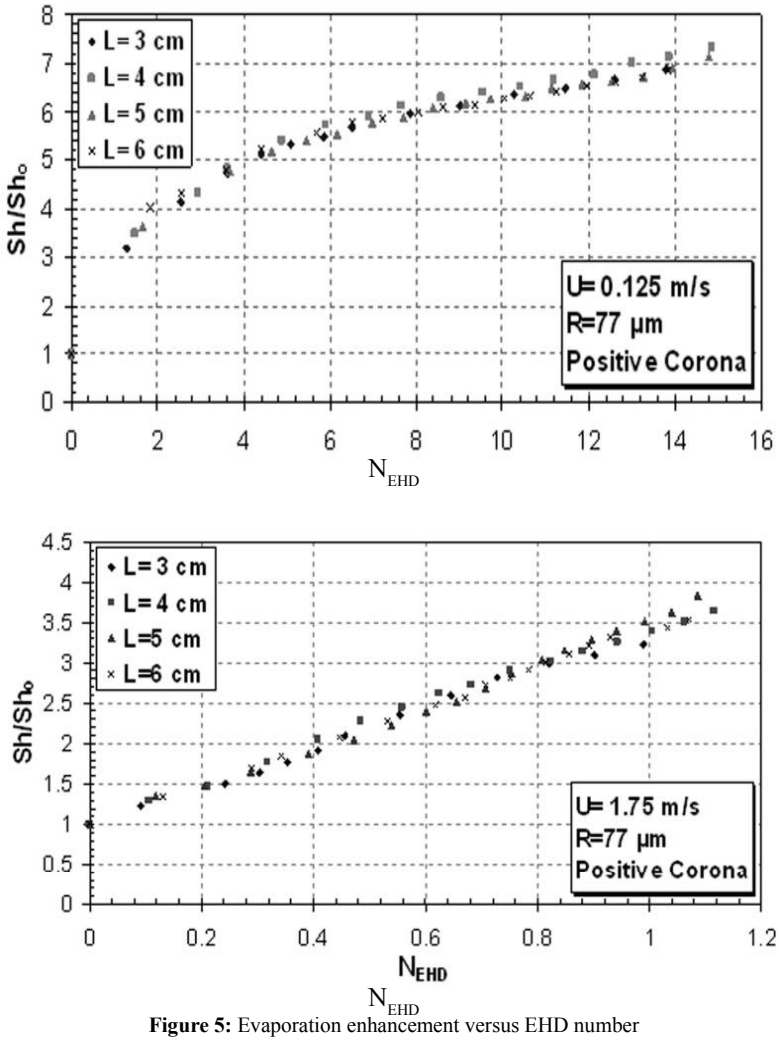

Figure 5: Evaporation enhancement versus EHD number

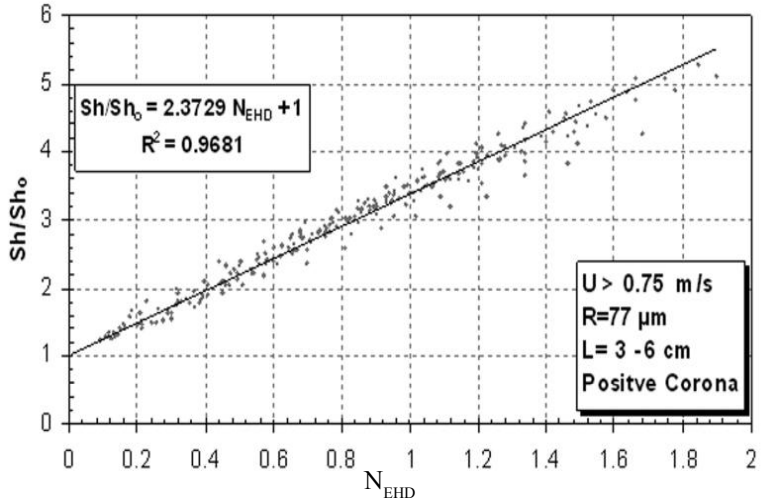

Figure 6: Evaporation enhancement versus EHD number

The values of the evaporation enhancement for all the electrode spacings and air velocities over 0.75 m.s^{-1} are presented in Figure 6. It is observed that the evaporation enhancement can be very well correlated as a linear function of EHD number. In this case, the results can be correlated using the following form:

$$\frac{Sh}{Sh_0} = 1 + a\, N_{EHD} \tag{12}$$

where, a is a constant determined by the correlation. In this form, the evaporation enhancement is reduced to unity when no electric field is applied and in the presence of electric field, it increases linearly with the increase of EHD number. The equation of the regulation line is given by:

$$\frac{Sh}{Sh_0} = 1 + 2.37\, N_{EHD} \tag{13}$$

Electrohydrodynamics known as a novel low energy consumption technique can be an outstanding method for increasing the rate of the heat and mass transfer. Figure 7 shows the evaporation enhancement as a function of electric power consumption for the air flow velocities of 0.125 and 1.75 m.s^{-1} and different electrode spacings. Applying electric field with a very small amount of energy usage can lead to a great evaporation enhancement especially at low air flow velocities. For instance, at an air velocity of 0.125 m.s^{-1} and an electrode spacing of 3 cm, the evaporation enhancement is 3.2 by consuming 0.071 W electrical power which reduces to 1.2 as the air velocity increases to 1.75 m.s^{-1}.

The evaporation enhancement increases steeply at low electrical powers and gently at higher electrical powers, which highlights the effect of electric field at lower power consumptions. The results also show that while the evaporation enhancement is a function of air flow velocity, it is nearly independent of electrode spacing for fixed electrical power consumption. In other words, when electrical power consumption is a matter, electrode spacing is insignificant.

The performance of electrohydrodynamic technique is defined here as the ratio of an increase in the heat absorbed by the evaporated water in the presence of electric field to the electrical power consumption (VI) as reads:

$$P_e = \frac{(\dot{m}_{eva} - \dot{m}_{eva_0})\lambda}{VI} \tag{14}$$

where, $\dot{m}_{eva}$ and $\dot{m}_{eva_0}$ are the rate of water evaporation with and without electric field respectively. λ also stands for the latent heat of evaporation of water.

As shown in Figure 8, the performance of electrohydrodynamic water evaporation decreases with the increase of applied voltage and the decrease of electrode spacing. However, these results should not be confused with the earlier results presented in Figure 3, which show that the evaporation enhancement increases by increasing the applied voltage and decreasing the electrode spacing.

Figure 8 implies that electrical energy is more effectively used at a lower applied voltage and the performance falls down sharply for higher voltages.
As it is seen, the EHD performance value like the evaporation enhancement value is a function of both corona wind velocity and axial air flow velocity; so, it seems to be possible to correlate the value of EHD performance to corona wind and axial air flow velocity. This has been performed in Figure 9. In this figure, the performance values for air velocities over 0.75 m.s^{-1} and different electrode spacings are plotted. As it can be seen, they can be correlated very well by the following equation:

$$P_e = \frac{12.4}{(U_e^{\,1.4622} \times U^{0.5})} \qquad U > 0.75\ m/s \tag{15}$$

According to the previous statements, this equation shows that corona wind is more effective at lower air velocities.

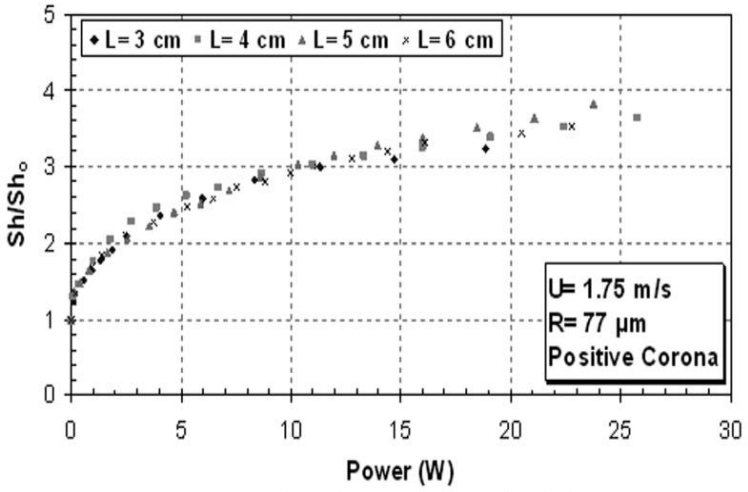

Figure 7: Evaporation enhancement versus electrical power

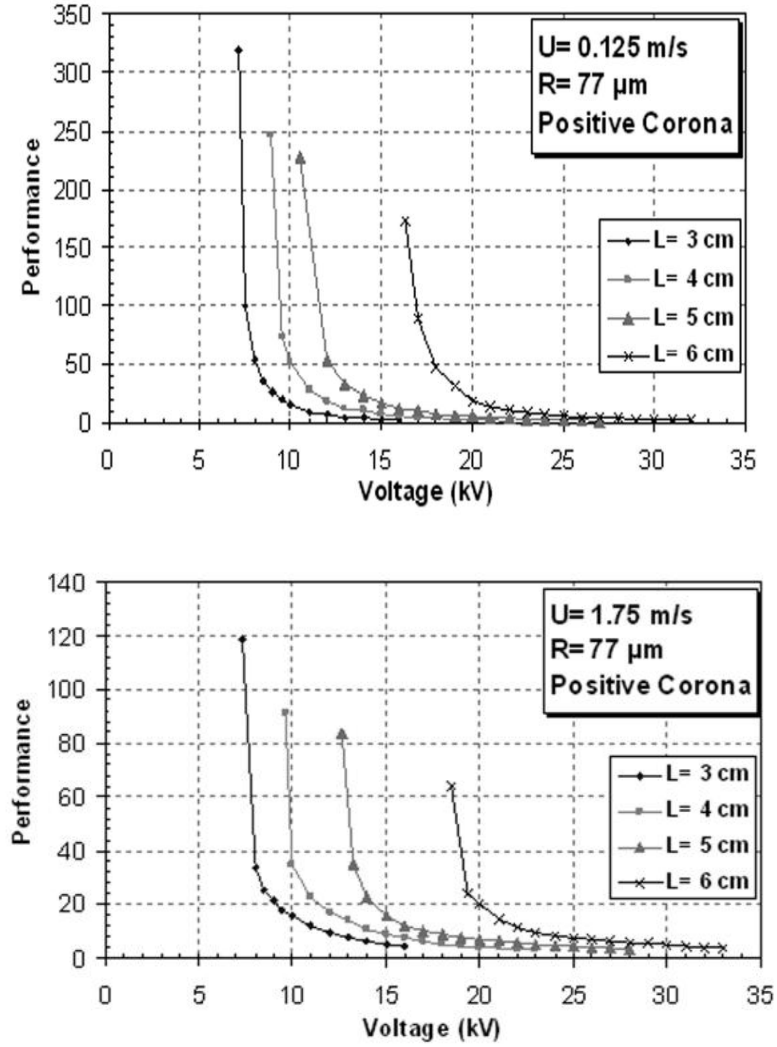

Figure 8: EHD Performance versus voltage

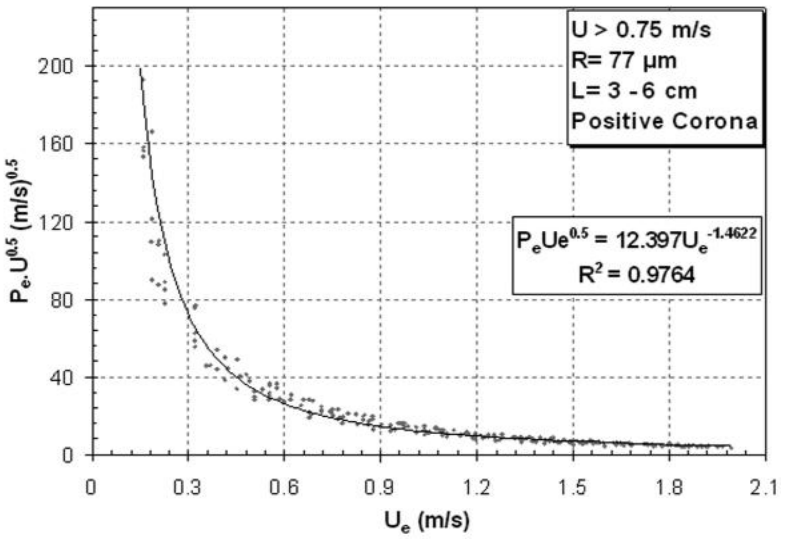

Figure 9: EHD Performance versus corona wind velocity

Conclusion

This experimental work revealed the level of the evaporation enhancement that can be achieved by corona wind in the wind tunnel. The effects of corona wind velocity, electrode spacing, and air flow velocity on the evaporation enhancement have been examined. The emitting electrode was a thin cooper wire suspended above a cooper plate and charged with positive DC high voltage. The results could be summarized as follows:

• The evaporation enhancement increases by increasing voltage while decreases as the electrode spacing increases at a fixed voltage.
• It is found that as the air flow velocity over the water surface increases, the EHD enhancement reduces, which implies that EHD effectiveness on the evaporation enhancement gradually diminishes by increasing the air flow velocity. The maximum enhancement was 7.3 and obtained at an air velocity of 0.125 $m.s^{-1}$.
• It can be deduced that the evaporation enhancement is nearly independent of electrode spacing at a fix corona wind velocity. This result strengthens the postulation that corona wind velocity is the main mechanism in the evaporation enhancement.
• Except for very low air flow velocities, the evaporation enhancement is a linear function of EHD number.
• The performance of EHD evaporation decreases by increasing the applied voltage. However, this should not be confused with the earlier statement denoting that the evaporation rate increases with the applied voltage. What actually is emphasized here is that the electrical energy usage is more effective at a lower applied voltage.
• Electrohydrodynamic technique by applying a very small amount of energy can lead to a great level of enhancement, especially at voltages near corona inception voltage.

Nomenclature

A: plate electrode area (m^2)
b: positive ion mobility $(1.43 \times 10^{-4}\ m^2/Vs)$
C: water vapor concentration (Kg_w/m^3)
T: wet bulb temperature (° C)
D: mass diffusion of water vapor (m^2/s)
d: characteristic length (m)
E: electric field intensity (V/m)
F_e: electrohydrodynamic force (N/m^3)
h_m: mass transfer coefficient (m/s)
I: electric current (A)
L: electrode spacing
$\dot{m}_{eva}$: rate of water evaporation with electric field (Kg_w/s)
$\dot{m}_{eva_0}$: rate of water evaporation without electric field (Kg_w/s)
$\dot{m}_{dry\,air}$: mass flow rate of dry air (Kg_a/s)
p: atmospheric pressure (kpa)
p_e: electrohydrodynamic performance (kg/kj)
p_g: saturated pressure of water vapor (kpa)
Sh: dimensionless Sherwood number
U: axial air flow velocity (m/s)
U_e: corona wind velocity (m/s)
V: electrical voltage (V)
ρ_a: dry air density (Kg_w/m^3)
q_e: free electric charges density $(1/m^3)$
ε_0: electric permittivity of vacuum $(8.85 \times 10^{-12}\ F/m)$
ω: humidity ratio (Kg_w/Kg_a)
ϕ: relative humidity

References

[1]. Laohalertdechaa S., Naphonb P., and Wongwises S., "*A Review of Electrohydrodynamic Enhancement of Heat Transfer*", Renewable and Sustainable Energy Review, Vol. 11, pp. 858–876, 2007.
[2]. Molki M., and Bhamidipati K., "*Enhancement of Convective Heat Transfer in the Developing Region of Circular Tubes Using Corona Wind*", International Journal of Heat and Mass Transfer, Vol. 47, pp. 4301–4314, 2004.
[3]. Sadek H., Robinson A. J., Cotton J. S., Ching C. Y., and Shoukri M., "*Electrohydrodynamic Enhancement of In-tube Convective Condensation Heat Transfer*", International Journal of Heat and Mass Transfer, Vol. 49, pp. 1647–1657, 2006.
[4]. Alemrajabi A., and Lai F. C., "*EHD-enhanced Drying of Partially Wetted Glass Beads*", Drying Technology, Vol. 23, pp. 597–609, 2005.
[5]. Goodenough T. I. J., Goodenough P. W., and Goodenough S. M. "*The Efficiency of Corona Wind Drying and its Application to the Food Industry*", Journal of food Engineering, Vol. 80, pp. 1233-1238, 2007.
[6]. Lai F. C., Huang M., and Wong D. S., "*EHD-Enhanced Water Evaporation"*, Drying Technology, Vol. 22, pp. 595–606, 2004.
[7]. Lai, F. C., and Sharma, R. K., *"EHD-enhanced Drying with Multiple Needle Electrodes"*, Journal of Electrostatics, Vol. 63, pp. 223–237, 2005.
[8]. Chen Y. H., and Barthakur N. N., *"Electrohydrodynamic Drying of Potato Slabs"*, Journal of Food Engineering, Vol. 23, pp. 107–119, 1994.
[9]. Barthakur N.N., *"Electrohydrodynamic Enhancement of Evaporation from NaCl Solutions"*, Desalination, Vol. 78, pp. 455–465, 1990.
[10]. Shakouri Pour M., and Esmaeilzadeh E., *"Experimental Investigation of Convective Heat Transfer Enhancement from 3D-shape Heat Sources by EHD Actuator in Duct Flow"*, Experimental Thermal and Fluid Science, Vol. 35, pp. 1838–1891, 2011.
[11]. Atalık K., and Snmezler U., *"Heat Transfer Enhancement for Boundary Layer Flow over a Wedge by the Use of Electric Fields"*, Applied Mathematical Modeling, Vol. 35, pp. 4516–4525, 2011.
[12]. Rashkovan A., Sher E., and Kalman, H. *"Experimental Optimization of an Electric Blower by Corona Wind"*, Applied Thermal Engineering, Vol. 22, 1587–1599, 2002.
[13]. Stuetzer M., *"Ion Drag Presuure Generation"*, Journal of Applied Physics, Vol. 30, pp. 984-994, 1959.

[14]. Kamkari B. *Experimental Investigation of Water Evaporation Enhancement Using Electrohydrodynamics*, M.Sc. Thesis, Department of Mechanical Engineering, Isfahan University of Technology, 2008.
[15]. Sadek, S., Fax, E., Hurwitz, M., "*The Influence of Electric Fields on Convective Heat and Mass Transfer from a Horizontal Surface under Force Convection"*, Journal of Heat Transfer, Vol. 94, pp. 144-148, 1972.